BRAIN COMMUNICATIONS

Corticoperipheral neuromuscular disconnection in obstructive sleep apnoea

Haralampos Gouveris,[1] Katharina Bahr,[1] Elena Schmitt,[1,2] Ali Abriani,[1,2] Tjarko Boekstegers,[1,2] Sanja Fassnacht,[1,2] Tilman Huppertz,[1] Sergiu Groppa[2] and Muthuraman Muthuraman[2]

The roles of central nervous mechanisms and cortical output in obstructive sleep apnoea remain unclear. We addressed corticomuscular coupling between cortical sensorimotor areas and lower facial motor units as a mechanistic pathway and as a possible surrogate marker of corticoperipheral motor control in obstructive sleep apnoea. In this exploratory cross-sectional retrospective study, we analysed EEG (C3 and C4 leads) and chin EMG from polysomnography recordings in 86 participants (22 females; age range: 26–81 years): 27 with mild (respiratory disturbance index = 5–15 events/h), 21 with moderate (15–30 events/h) and 23 with severe obstructive sleep apnoea (>30 events/h) and 15 control subjects (<5 events/h). By computing C3-/C4-EEG–chin EMG coherence of signal dynamics in time and frequency domains, we investigated corticomuscular coupling between cortical sensorimotor areas and lower facial motor units with increasing obstructive sleep apnoea severity during the entire sleeping time, during different sleep stages and during obstructive respiratory events, including 5 s before (stable breathing) and after events (breathing resumption). In addition, we studied a possible influence of body mass index and autonomic nervous system activation. We found that both average and respiratory event-specific corticomuscular coupling between cortical sensorimotor areas and lower facial motor units weakened significantly with increasing obstructive sleep apnoea severity, was strongest during N3 and weakened in N1, N2 and rapid eye movement stages (in decreasing order). Coupling increases significantly during the obstructive respiratory events compared with coupling just before and following them. Results were independent of body mass index or autonomic nervous system activation. We conclude that obstructive respiratory events in obstructive sleep apnoea are very strongly associated both quantitatively and temporally with the degree of disconnection within the cortical sensorimotor areas—lower facial motor units pathway. This quite coordinated activity pattern suggests a cortical sensorimotor area-driven obstructive respiratory event pattern generator and a central motor output disorder in obstructive sleep apnoea.

1 Sleep Medicine Center and Department of Otolaryngology, University Medical Center of Johannes Gutenberg University Mainz, 55131 Mainz, Germany
2 Movement Disorders and Neurostimulation, Biomedical Statistics and Multimodal Signal Processing Unit, Department of Neurology, University Medical Center of Johannes Gutenberg University Mainz, 55131 Mainz, Germany

Correspondence to: Muthuraman Muthuraman, PhD, Movement Disorders and Neurostimulation
Biomedical Statistics and Multimodal Signal Processing Unit, Department of Neurology
University Medical Center of Johannes Gutenberg University Mainz, Langenbeckstrasse 1, 55131 Mainz, Germany
E-mail: mmuthura@uni-mainz.de

Keywords: cortical; motor; neuromuscular; coupling; obstructive sleep apnoea

Received February 3, 2020. Revised March 31, 2020. Accepted April 13, 2020. Advance Access publication May 11, 2020

Abbreviations: CM = corticomuscular; CSMA = cortical sensorimotor areas; ORE = obstructive respiratory event; OSA = obstructive sleep apnoea; PSG = polysomnography; RDI = respiratory disturbance index; REM = rapid eye movement; ROC = receiver operating characteristic curve

Graphical Abstract

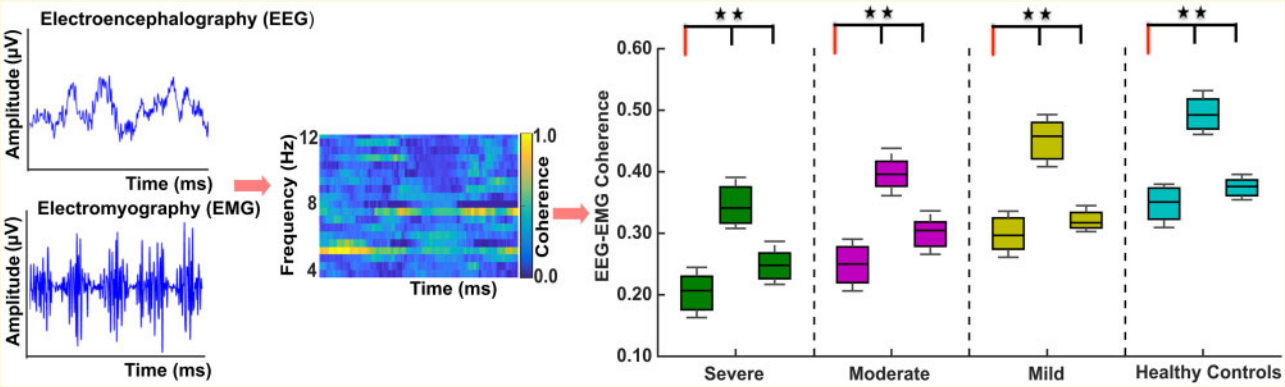

Introduction

Given that obstructive apnoeas and hypopnoeas occur only during distinct brain states (i.e. sleep, anaesthesia) and cerebral disease (e.g. stroke), central neural mechanisms may play a role in driving peripheral upper airway muscular output. Corticomuscular (CM) coherence quantitatively depicts CM coupling and is used as a neurophysiologic marker of cortical locomotor drive to peripheral motor output units (Mima and Hallett, 1999). Weakening of CM coupling is a major mechanism underlying voluntary muscle fatigue, with associated motor performance impairment (Yang *et al.*, 2009). Patients with idiopathic rapid eye movement (REM) sleep behaviour disorder show increased CM coherence between sensorimotor cortex EEG and chin muscle EMG during REM sleep (Jung *et al.*, 2012). Therefore, involuntary activity of the chin (lower facial) muscles, which exhibit voluntary activity during wakefulness, may be useful in assessing CM coherence during sleep. In addition, brief recruitment of submental muscles with transcranial magnetic stimulation (Massimini *et al.*, 2007; Melo-Silva *et al.*, 2013*a*) and consecutive twitch of submental muscles (Melo-Silva *et al.*, 2013*b*) during sleep improve upper airway mechanics, maximal inspiratory flow and inspiratory volume of flow-limited cycles.

Patients with obstructive sleep apnoea (OSA) show neuromuscular dysfunction of upper airway dilator muscles, especially genioglossus, which exhibits neurogenic changes in its motor unit potential waveforms similar to those seen in neuropathies (Saboisky *et al.*, 2012). CM coupling has not been studied systematically in OSA and studies on CM coupling between central cortical sensorimotor areas (CSMAs) and lower facial motor units in OSA have not been reported so far. Lower facial motor units may (directly or indirectly) influence upper airway patency during sleep. Chin surface EMG captures activity of the ventral digastric and/or mylohyoid or mentalis muscles, which receive motor input from trigeminal, hypoglossal and facial nerves. Healthy sleepers have a mentalis muscle-associated REM atonia index of 100% (Frauscher *et al.*, 2014). Hence, chin EMG may detect even minor activity changes in sleep disorders. Standard polysomnography C3- and C4-EEG-electrode locations depict motor cortex activity (left and right M1, respectively) (Carbonnell *et al.*, 2004).

Based on these findings, in this exploratory study, we compared CM coupling between CSMA and lower facial motor unit among sleep stages and among different OSA severity patient groups and tested whether the CM-coupling metric could classify OSA severity. In addition, we did a targeted investigation of the CM coupling during the course of apnoeas and hypopnoeas and 5 s before (stable breathing) and after the events (breathing resumption), to explore any event-related abrupt changes in CSMA drive to the periphery. To further test the reproducibility of our findings, we performed the analyses on recordings of two consecutive nights of sleep study. Promoting understanding of the connectivity between cortical regions and peripheral cranial nerves and cranio-cervical musculature could provide a framework to study relevant pathophysiologic questions in patients with OSA with or without neurological comorbidities (Gouveris and Eckert, 2018; Somboon *et al.*, 2019).

Materials and methods

Study design and participants

In this exploratory study, we retrospectively analysed the polysomnographic (PSG) recordings of 86 adults (22

females; age range: 26–81 years) who were tested during two consecutive nights in the sleep laboratory of a tertiary hospital because of a suspicion of sleep-disordered breathing. Data of patients with concomitant narcolepsy, hypersomnia, restless leg syndrome, circadian sleep disorder, a psychiatric or neurologic (peripheral or central) disorder, heart failure, history of myocardial infarction, chronic obstructive pulmonary disease and history of malignant diseases were excluded. Data of patients treated with benzodiazepines, gamma-aminobutyric acid (GABA) receptor agonists, antidepressants or opiates were excluded because of their effect on EMG and EEG. Data of patients with known alcohol abuse were excluded from analysis. Alcohol consumption before PSG was excluded by history. Patients with continuous positive airway pressure or auto-titrating positive airway pressure therapy, dental appliance or soft-tissue surgery for OSA were excluded.

All individuals had undergone overnight polysomnography (PSG) according to the American Academy of Sleep Medicine standards in our accredited sleep laboratory. Sleep stages and respiratory events were manually scored according to the American Academy of Sleep Medicine 2012 scoring guidelines (Berry *et al.*, 2012).

Polysomnographic measurements and scoring

Polysomnographic recordings involved C3- and C4-EEG recordings, electrooculogram, submental and bilateral pretibial EMG and one-lead electrocardiogram. Nasal airflow was detected by measurement of impact pressure through a nasal sensor that determined pressure fluctuations of the breathed air stream. Thoracic and abdominal excursions by means of piezoelectric bands, oxyhaemoglobin saturation (using a pulse oxymeter) and body position were simultaneously recorded. Snoring was recorded with a pre-laryngeally fixed microphone. The polysomnographic recordings were performed using the Alice-LE-Diagnostic Sleep System (Philips Healthcare/Respironics, Best, Netherlands). In the morning following each sleep study night, sleep stages and sleep-related respiratory events were manually scored according to the American Academy of Sleep Medicine-2012 guidelines (Berry *et al.*, 2012). Nasal airflow amplitude reduction of the airflow signal 90%, lasting for at least 10 s, was defined as apnoea. Hypopnoea was defined as a reduction in the airflow signal on the nasal flow sensor between 30% and 90% of pre-event baseline for $\geq$10 s with an associated $\geq$3% reduction in the arterial blood oxygen saturation (SpO_2) and/or a cortical arousal. Apnoea events were further classified into obstructive, central or mixed based on simultaneous evaluation of nasal airflow and thoracic and abdominal excursion.

Approval for the study was provided by the local Institutional Review Board (Nr. 2018-13942). The research findings are based on research and clinical practices that conform to the principles of the Declaration of Helsinki.

Analysis of signal dynamics in time and frequency domains, coherence and phase estimation

EEG and EMG were sampled at 200 Hz and band-pass filtered (EMG 30–200 Hz; EEG 0.05–200 Hz). Each recording was segmented into a number of 1-s epochs ($L = 1000$), discarding all data segments with visible artefacts due to body movements or transient electrode recording artefacts. Depending on the length (N) of the recording and the data quality, 1-s epochs (M) were used for analysis, such that $N = LM$. The coherence spectrum was estimated using the Welch periodogram method (Welch, 1967). The statistical significance of the coherence at a particular frequency was calculated by (Halliday *et al.*, 1995):

$$1 - (1 - \chi)^{1/(M-1)},$$

where χ was set to 0.99, so that the confidence limit is $1 - 0.01^{1/(M-1)}$. Values of coherence above this confidence limit were considered to indicate a statistically significant linear correlation between the two time series, while values below this limit indicated the absence of correlation. Our next step was to analyse the dynamics of these frequency oscillations over time by applying the multitaper method for each recording (Muthuraman *et al.*, 2010). The dynamics of signals in the time and frequency domains were computed with the multitaper method (Mitra and Pesaran, 1999). The phase spectrum $\hat{\varphi}(\omega)$ was estimated by taking the argument of the cross spectrum (Halliday *et al.*, 1995) in which ω represents the frequency.

Multitaper method used for polysomnographic (PSG) signal analysis

In this method, the spectrum was estimated by multiplying the data with K different windows (i.e. tapers). The complete description of the method is explained elsewhere (Muthuraman *et al.*, 2010). The time step was 50 ms with overlapping windows of 1000 ms, providing an approximate time resolution of 50 ms and an approximate frequency resolution of 1 Hz. In a further analysis, all initial coherence estimates of the individual EEG electrodes averaged over (1–100 Hz) were combined to get a pooled coherence estimate. This can be done by computing the individual second-order spectrum using a weighting scheme and estimating the coherence to obtain the pooled estimate of the two EEG (C3 and C4) electrodes (Rosenberg *et al.*, 1989; Amjad *et al.*, 1997).

Spectral estimation for very short data intervals

For the spectral estimation, we applied the multitaper coherence method, which uses more than one window (taper) for signal analysis. This recently introduced method also performs with high temporal resolution irrespective of the frequency bands under study (Muthuraman *et al.*, 2018). For the present study, it is important to detect even very short (e.g. 5-s) time intervals during which the coupling in a specific frequency range drops or disappears.

Treatment of artefacts of the polysomnographic (PSG) signals

The PSG data were directly subjected to independent component analyses (FastICA) (Oostenveld *et al.*, 2011) to remove the components representing the muscle artefacts, eye blinks, eye movements and line noise. On average 6 of 32 components (3 ± 2.6, mean $\pm$ standard deviation) were rejected, 1–2 were related to the eye artefacts (1 ± 0.68), 1–2 were related to line noise (1 ± 0.34) and 1–2 were related to muscle artefacts (1 ± 0.24). The residual muscle artefacts were visually inspected, removed and interpolated with the cubic interpolation method. A fourth-order Butterworth low-pass filter with a cut-off frequency of 200 Hz was applied to avoid aliasing, which was followed by a band-pass filtered separately for EEG and EMG signals.

Statistical analysis

The entire PSG signals of all patients were used for analysis. Statistical analysis was performed with MATLABR 2015a. The demographic patient data were compared among the four groups using a one-factorial analysis of variance (ANOVA), with group as the factor. To investigate whether sleep stages were associated with changes in CM coupling in a consistent manner, we calculated CM coupling in the various sleep stages in each disease severity group, using the two-factorial ANOVA (the group was one factor and sleep stages were the second factor). To test whether CM coupling may be used as a surrogate marker to predict disease severity [using respiratory disturbance index (RDI) = 15/h as cut-off], the area under the curve value was calculated for each receiver operating characteristic curve (ROC).

Receiver operator characteristic (ROC) analyses

A classifier is a parameter or a variable with a suitable optimal threshold, which is used in a classification algorithm. In this study, only binary classification was considered, e.g. classification between two different cases termed 'positive case' and 'negative case'. The performance of a classifier was evaluated by three main metrics—specificity, sensitivity and accuracy (Rangayyan, 2001).

We also investigated whether any significant correlations existed between the collected parameters. To this end, Spearman Rho coefficients were calculated. The Bonferroni correction was done for multiple comparisons. Disease severity classification was based on RDI values. In a control experiment, we looked separately at the EMG power and EEG power to differentiate between the disease severity groups.

We studied EEG–EMG coherence during obstructive respiratory events (OREs), 5 s before the event (stable breathing) and 5 s after the event (breathing resumption). We also performed this detailed analysis of the EEG–EMG coherence at each sleep stage in each one of the patient groups separately, to test if there was a sleep-stage-specific effect.

To study a possible correlation with autonomic nervous system activation, we correlated EEG–EMG coherence in the time domain with the respective heart rate (beats per minute) recorded on polysomnography as a measure of autonomic alterations. We also analysed the association between body mass index and the EEG–EMG coherence metric in each one of the patient groups. To further test for specificity of the EEG–chin EMG coherence metric, we analysed separately the coherence between EEG and tibialis muscle (leg) EMG signals. We also tested the specificity of the observed changes by doing additional analyses of the simultaneous activation pattern of the thoracic respiratory muscles, as provided by the thoracic excursion signals during polysomnography.

To further test the reproducibility of our findings, we performed the same analyses on the polysomnographic recordings of two consecutive nights of sleep study of the same individuals (patients with OSA and controls).

Data availability

The data that support the findings of this study are available from the corresponding author, upon reasonable request.

Results

PSG recordings of 86 eligible adult participants were included for analysis. Twenty-seven patients had mild (RDI = 5–15/h), 21 patients had moderate (RDI $\geq$ 15/h and <30/h) and 23 patients had severe OSA (RDI $\geq$ 30/h). Fifteen patients with RDI <5/h were the control group. Demographic characteristics and PSG variables are displayed in Table 1. Age and average SpO_2 were not significantly different between the four groups ($P > 0.05$). All the other between-group *post hoc* comparisons were significantly different ($P < 0.001$, see Table 1 for details). CM coupling was reduced in patients with OSA

Table 1 Clinical demographics and sleep-associated variables in the various groups of the study participants

	Age	Sex	BMI	RDI	ODI (non-REM)	ODI (REM)	T90 (SpO2)%	Arousal index
Healthy	56.24 ± 10.27	M (11), F (4)	18.90 ± 2.82	2.49 ± 1.52	1.93 ± 1.81	4.38 ± 528	0.14 ± 0.23	17.24 ± 8.82
Mild OSA	54.78 ± 11.67	M (22), F (5)	25.43 ± 3.06	11.50 ± 3.36	5.86 ± 2.14	10.29 ± 11.04	0.92 ± 0.02	19.39 ± 3.29
Moderate OSA	54.44 ± 8	M (17), F (4)	27.04 ± 3.67	22.61 ± 4.21	11.01 ± 7.91	13.90 ± 13.22	3.11 ± 0.03	24.62 ± 6.39
Severe OSA	58.08 ± 13.07	M (19), F (4)	29.98 ± 5.83	53.61 ± 23.07	39 ± 30.02	29.51 ± 24.32	10.30 ± 0.36	37.66 ± 17.50
(ANOVA factor group); *P*-values	(*F*(3,6.39) = 3.45; *P* > 0.05)	(*F*(3,4.87) = 2.97; *P* > 0.05)	(*F*(3,1.29) = 89; *P* < 0.01)	(*F*(3,0.84) = 2305; *P* < 0.001)	(*F*(3,1.98) = 453; *P* < 0.001)	(*F*(3,2.08) = 29; *P* < 0.01)	(*F*(3,0.78) = 206; *P* < 0.001)	(*F*(3,0.70) = 7365; *P* < 0.001)

Depicted are age (years), sex of the participants, BMI (kg/m^2) and the RDI (in respiratory events/h sleep). Respiratory events include apnoeas, hypopnoeas and respiratory effort-related arousals. Healthy individuals had RDI ≤ 5 events/h sleep, patients with mild OSA had RDI = 5–15/h sleep, patients with moderate OSA had RDI = 15–30/h sleep and patients with severe OSA had RDI > 30/h sleep. Numerical values are means followed by standard deviations. All numerical values are rounded up to the second decimal point. The arousal index was significantly different between the severe OSA versus all the other three groups ($P < 0.001$), but not between the other groups. BMI was not significantly different between mild versus moderate ($P = 0.963$) and moderate versus severe ($P = 0.119$), whereas all other comparisons were significant ($P < 0.001$).
Arousal index = number of arousals/h sleep; BMI = body mass index; ODI = oxygen desaturation index, in events/h sleep; t90 = percentage of sleep time during which blood oxygen saturation is <90%.

compared to healthy controls. There was a positive correlation between the degree of RDI-based OSA severity and the degree of CM-coupling reduction. Moreover, CM coupling followed a very consistent sleep stage pattern in all disease severity groups. The findings were quite robust during both nights of sleep study.

Using EEG–EMG coherence to classify OSA severity

Given that the cut-off RDI of 15/h significantly influences clinical therapeutic decisions, we used this value to test if the EEG–EMG coherence metric could differentiate between patients with and without clinically significant OSA. The respective ROC (receiver operating characteristic) curves are shown in Fig. 1 (and in Supplementary Fig. 1). There were quite significant differences in EEG–EMG coherence between patients with RDI >15/h and patients with RDI <15/h (area under the curve = 0.843, $P < 0.0001$ for the first night of sleep study and area under the curve = 0.892, $P < 0.0001$ for the second night of sleep study). In a control experiment using only the EEG pooled (EEG C3 and C4 signals) average power and the EMG average power, we could not distinguish between disease severity groups (area under the curve < 0.5, $P > 0.05$).

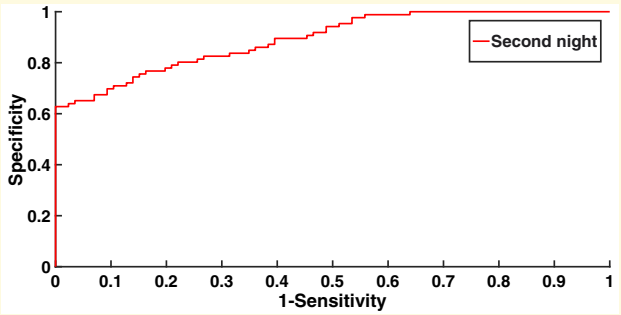

Figure 1 ROC curve analysis of EEG–EMG coherence in OSA severity subgroups. ROC curve analyses for the EEG–EMG coherence metric for the comparison between the group of individuals with RDI >15/h (moderate and severe OSA) and the group with RDI <15/h from the second night of sleep study. Depicted is the calculated curve. ROC = receiver operator characteristic.

Temporal pattern of EEG–EMG coherence during, just before and just after the OREs

A significant increase (peak) in CM coupling was detected during the course of OREs (apnoeas and hypopnoeas) (Fig. 2). The absolute values of this CM-coupling peak decrease with increasing OSA severity. Regardless of severity, CM coupling quite consistently weakened immediately before (5 s of stable breathing) and immediately after the OREs (5 s of breathing resumption). Within the same disease severity group, CM disconnection was the highest just before the OREs. Corticoperipheral disconnection during, just before and just after the OREs increased significantly with increasing OSA severity (Fig. 2). This pattern was quite reproducible and consistent during both study nights (Supplementary Fig. 2).

Corticomuscular EEG–EMG coherence during various sleep stages

CM coupling shows a specific, stable pattern during the distinct sleep stages, with N3 showing the highest CM coupling, followed by N1, N2 and REM. This pattern was quite reproducible in all four OSA severity groups and during both nights (Fig. 3 and Supplementary Fig. 3). Moreover, we could show clearly the sleep stage-associated influence on the EEG–EMG coherence findings within each OSA severity group (Fig. 4).

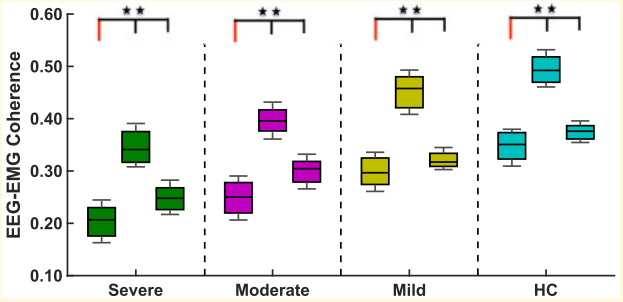

Figure 2 EEG–EMG coherence in various OSA severity patient groups. Comparison of EEG–EMG coherence between groups (mild, moderate and severe obstructive sleep apnoea, HC). Dashed lines separate the four different OSA severity groups of individuals of the second night of sleep study. The first box plot in each group represents coherence values during the time window 5 s before the beginning of the ORE (stable breathing). The second box plot in each group represents coherence values during the respiratory event, and the third box plot represents coherence values during the time window 5 s after completion of the respiratory event (breathing resumption). The statistics are represented based on the comparison between the red line marked group and the other groups as black lines. The ** indicates a significance of ($P < 0.001$). The factor 'group' was significant ($F(3,360) = 4983$; $P < 0.001$), and the factor 'events' was also significant ($F(2,1198) = 387$; $P < 0.001$). We also found a significant interaction between these two factors ($F(6,1198) = 49$; $P < 0.001$). The *post hoc* tests for all comparisons were significant ($P < 0.01$). The factor group was significant ($F(3,290) = 2834$; $P < 0.001$), and the factor events was also significant ($F(2,1029) = 428$; $P < 0.001$). A significant interaction between these two factors ($F(6,1029) = 37$; $P < 0.001$) was found. The *post hoc* tests for all comparisons were significant ($P < 0.01$). The number of subjects in each group was mild (27), moderate (21), severe (23) and healthy controls (15). HC = healthy control.

Autonomic nervous system activation and BMI do not influence CM coupling in OSA

We found no significant Pearson correlation between heart rate and EEG–EMG coherence in any of the patient severity groups or controls tested (Supplementary Figs 4–7). Therefore, a major autonomic activation metric (heart rate) is not influenced by activity of the CSMA–lower facial motor units (LFMU) pathway. We also found no significant correlation between body mass index and the EEG–EMG coherence in any one of the four patient groups (Supplementary Figs 8–11).

Corticoperipheral disconnection is cervical muscle specific in OSA

We found no significant coherence between EEG and leg EMG signals in any of the patient groups or sleep stages tested. This clear dissociation between the EEG–leg EMG coherence metric and EEG–chin EMG coherence metric provides a further argument supporting a specific role of the CSMA–lower facial motor unit (central sensorimotor area–lower facial motor units) pathway in the control of breathing during sleep.

Dissociation between cervical and thoracic muscle activation in OSA

The variance of the phase difference between the EEG sensorimotor cortex signals and the activation of the thoracic respiratory muscles, as depicted by the thoracic excursion signals on PSG, diminishes significantly with increasing OSA severity (Fig. 5). We interpret this quite robust and reproducible finding as a compensatory (central-driven) mechanism to ensure breathing stability with increasing severity of obstruction.

Discussion

Our findings provide evidence that average CM coupling between central CSMAs and lower facial (especially mentalis muscle) motor units weakens progressively with increasing OSA severity. More importantly, this progressive CM disconnection was also specifically detected during the OREs and was increasing with increasing OSA severity. Regardless of OSA severity, CM coupling decreases just before (i.e. during apparent stable breathing) and just after respiratory events (i.e. during breathing resumption), while reaching its peak during the ORE itself. Also, CM coupling was strongest in stage N3 and decreased in N1, N2 and REM stages, in decreasing order. All these patterns were quite robust during both sleep study nights (Supplementary Figs 1–3). These findings did not correlate neither with body mass index nor with autonomic nervous system activation. CM coupling is more sensitive for detecting OSA degree of severity than solely the average power of C3/C4-EEG signals or chin EMG signals alone, since the latter metrics alone are not able to separate OSA disease severity groups.

Clinical and translational implications

Both immediately before and immediately after the event CM coupling weakens, while during the event CM coupling peaks. This peak could be a compensatory mechanism to promote stable breathing during OREs in patients with OSA. This compensatory cortical output- or CM connectivity-based mechanism, with its emergent highest performance during the OREs, probably becomes insufficient with increasing OSA severity.

Increased or decreased CM coupling during the sleep stages may lay out evidence for the numerous stage-specific mechanisms controlling upper airway muscle function in OSA. This provides the basis for building a functional map of cortical projections to brainstem

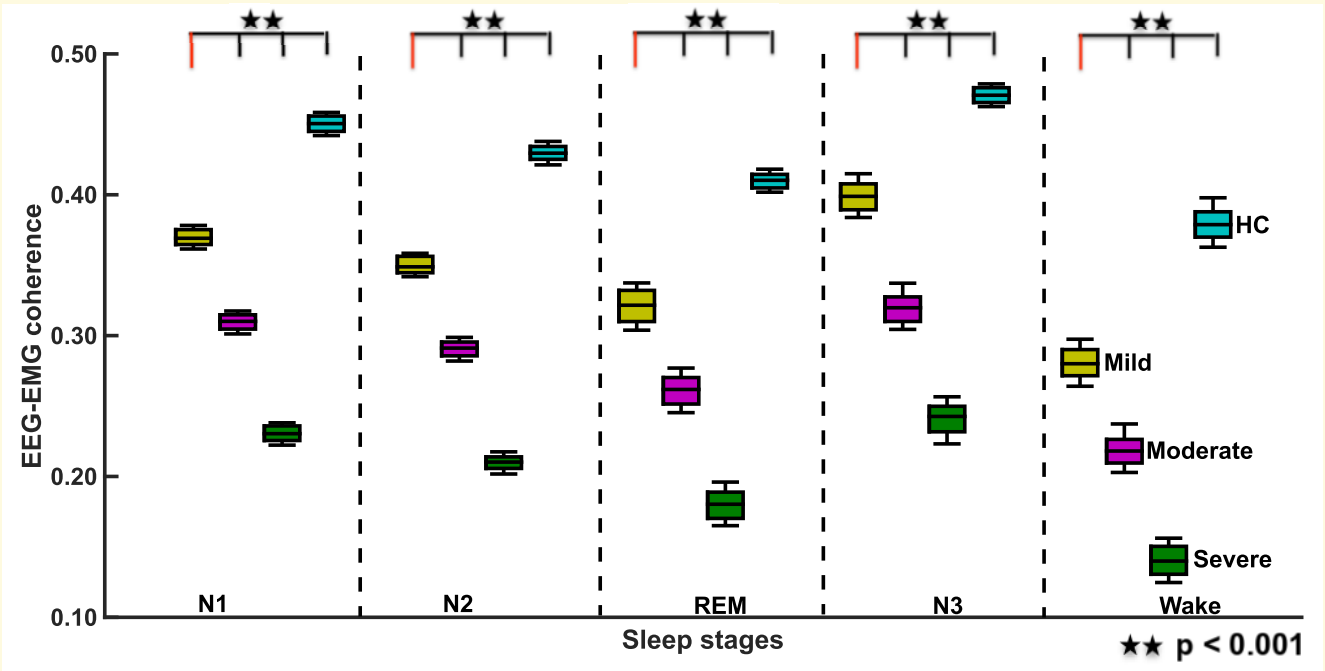

Figure 3 Sleep stage- and disease severity-dependent EEG–EMG coherence in OSA. Comparison of EEG–EMG coherence between groups (mild, moderate and severe obstructive sleep apnoea, HC individuals) of the second night of sleep study. Dashed lines separate the five different sleep stages N1, N2, N3, REM and wake. The statistics are represented based on the comparison between the red line marked group and the other groups as black lines. The ** indicates a significance of ($P < 0.001$). The factor group was significant ($F(3,404 = 56\ 491$; $P < 0.001$), and the factor sleep stages was also significant ($F(4,1616) = 8075$; $P < 0.001$). We also found a significant interaction between these two factors ($F(12,1616) = 38$; $P < 0.001$). The *post hoc* tests for all comparisons were significant ($P < 0.01$). The factor group was significant ($F(3,385) = 6574$; $P < 0.001$), and the factor sleep stages was also significant ($F(4,1547) = 7639$; $P < 0.001$). A significant interaction between these two factors ($F(12,1547) = 46$; $P < 0.001$) was found. The *post hoc* tests for all comparisons were significant ($P < 0.01$). The number of subjects in each group was mild (27), moderate (21), severe (23) and HCs (15). HC = healthy control.

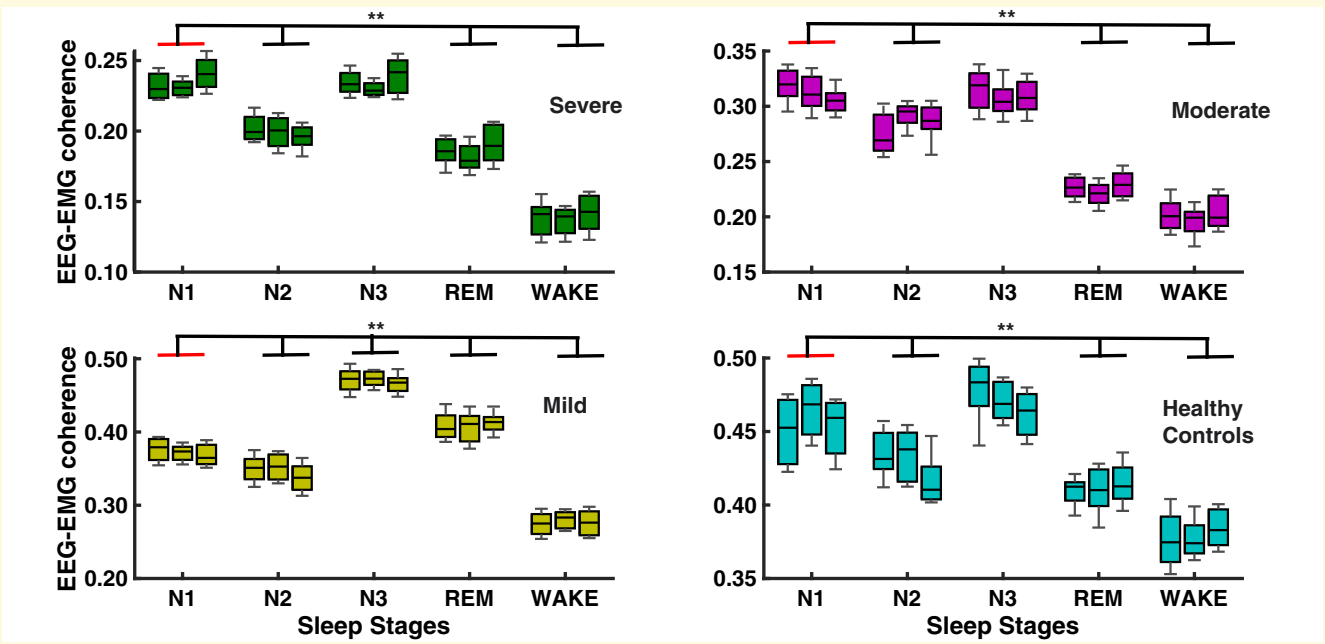

Figure 4 EEG–EMG coherence during the respiratory events in OSA. The EEG–EMG coherence box plots for each OSA severity group separately in each sub plot for all the five sleep stages (N1, N2, N3, REM and wake). In addition, the coherence was estimated based on the respiratory events, 5 s before, the respiratory event itself and the 5 s after the respiratory event. The ** indicates the $P < 0.01$. The number of subjects in each group was mild (27), moderate (21), severe (23) and healthy controls (15).

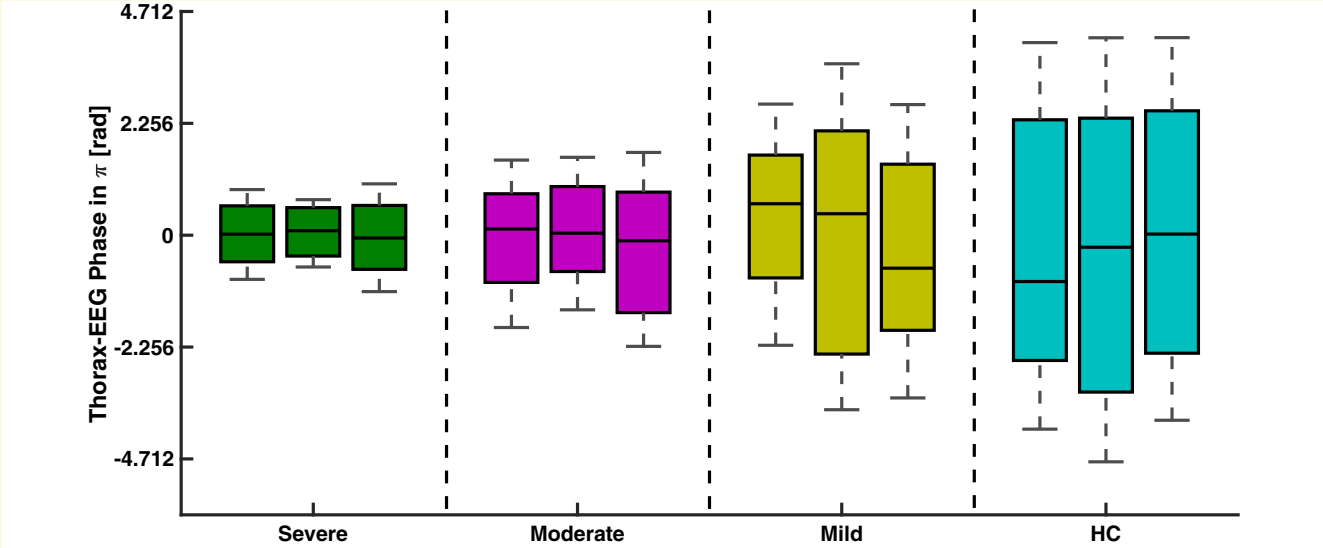

Figure 5 Disconnection between cortical motor output and thoracic muscle motor activation. The phase difference between the thoracic signal and the EEG in π radians for each OSA severity group separately. Calculations are based on the recordings of the second night of the sleep study. The number of subjects in each group was mild (27), moderate (21), severe (23) and healthy controls (15).

(pontine, in case of facial) motor neurons as a source of motor drive during the alternating sleep stages in patients with OSA. The finding that CM coupling is highest during N3 may explain the increased incidence of stable breathing and reduced incidence of OREs during N3 (Ratnavadivel *et al.*, 2009). This quite increased C3/C4 mentalis muscle CM coupling parallels the observed increased genioglossus activity found during slow wave sleep (McSharry *et al.*, 2013). In contrast, OREs occur much more frequently in N2 and even more prominently in REM than in other sleep stages (Ratnavadivel *et al.* 2010). Of note, during REM, occlusion occurs much more at the lower than at the more cranial parts of the upper airway (Boudewyns *et al.*, 1997). During phasic REM sleep, the human motor cortex exhibits an EEG pattern similar to the one observed when the motor cortex is activated (i.e. during voluntary movements) (De Carli *et al.*, 2016). Conversely, tonic REM sleep is characterized by EEG spectral values similar to those observed during relaxed wakefulness. Phasic REM sleep is characterized by higher EEG frequency values with respect to tonic REM sleep. Our results support this similarity between tonic REM and wakefulness (Fig. 3). The CM-coupling values we calculated for REM sleep were the average of both phasic and tonic parts. It will be interesting to test CM coupling in tonic and phasic REM sleep separately and also to restrict the study group to an REM phenotype of OSA to gain some new insight into the mechanisms of this specific OSA phenotype (Gabryelska and Białasiewicz, 2020).

Apart from the mentalis muscle, the posterior belly of the digastric muscle, the platysma, the depressor anguli oris and depressor labii inferioris muscles are all lower facial muscles innervated by the facial nerve. Activation of the digastric muscle causes elevation of the hyoid bone. If the hyoid is being held in place (by activation of the infrahyoid muscles), then the digastric muscle causes depression of the mandible and hence mouth opening. The platysma muscle depresses the mandible (and therefore also opens the mouth). The depressor anguli oris and the depressor labii inferioris when activated cause depression of the lower lip and enhance mouth opening. A parallel decrease in both phasic and tonic genioglossal activities is expected during mouth breathing (compared to nasal breathing), according to results observed in tracheostomized subjects, presumably due to local upper airway stimuli (Malhotra *et al.*, 2000).

Advancing these pathophysiologically relevant questions could contribute to the development of new therapeutic targets (e.g. pharmacological neuromodulation) in OSA. Moreover, patients with central neurological disorders (e.g. multiple sclerosis, epilepsy, Somboon *et al.*, 2019) could be characterized by developed analytical pathways and classified as at risk for developing OSA. The results could promote the development of new diagnostic testing modalities involving this metric and provide a framework to test breathing instability during sleep in a number of neurologic disorders using the raw data of the standard PSG recordings alone, without any need to record additional signals outside American Academy of Sleep Medicine standards. Brain or cranial nerve (e.g. hypoglossal nerve) stimulation paradigms may be developed to promote breathing stability during sleep using this metric as a feedback parameter.

CM disruption between sensorimotor cortex and lower facial musculature

CM coupling may be mediated by both ascending and descending pathways between brain and muscles. Oscillations may hold overt motor output constant to render the interpretation of the proprioceptive state more effective (Baker, 2007). Therefore, the decreased phasic/tonic muscle activity of the upper airway dilator muscles in OSA may contribute to the decreased proprioceptive afferent signal to the central motor areas (depicted by the C3- and C4-EEG leads) and hence to the decreased CM coupling in patients with OSA. More specifically, in our study, OREs were strongly associated with CSMA output. This observation involves not only the magnitude of this association but also a very coordinated activity coupling in the temporal domain. In addition, it was quite reproducible during both nights of sleep study. The combination of these associations (both quantitative and temporal) and its robust reproducibility during two consecutive nights of sleep increases the possibility of a CSMA-driven ORE pattern generator in OSA.

Methodological limitations and areas of future research

Given the anatomical inter-digitation and overlap between muscles in the lower facial area, it can be postulated that activity of any single lower facial muscle cannot be captured by a surface EMG electrode. In the present study, surface chin EMG may have captured EMG activity of many motor units of other parts of the lower facial musculature apart from the mentalis muscle, namely the depressor anguli oris, the depressor labii inferioris and the orbicularis oris inferior muscles (Lapatki *et al.*, 2006). EEG–EMG coherence methods have limitations as a means to assess the strength of the transmission of synaptic inputs into trains of motor unit action potentials. However, they still provide a relatively simple and reproducible way to tackle the problem of retrieving the embedded neural code from a surface EMG signal (Farina *et al.*, 2014). The possibility remains that the neural signals driving the coordinated lower muscle unit activity found in this study may be generated in a subcortical brain area (e.g. amygdala, thalamus or brainstem). In this case, PSG-recorded cortical C3/C4 activity may represent an after-signal or a 'cortical footprint' of the causative subcortical neural drive. It is technically unfeasible to measure such subcortical activity in humans using standard PSG. Nonetheless, the magnitude and temporal features of the CM-coupling metric found in our patients support that CSMA is the primary generator of patterned peripheral motor activity within this pathway.

Conclusions

These findings support the idea of a strongly associated (and possibly underlying) central motor disorder in OSA. Data from PSG signals used in this study are based on standard American Academy of Sleep Medicine methodology and hence are accessible to analysis in every accredited sleep laboratory. Future research may involve testing CM coupling using invasive measurements from intramuscular needle electrodes placed in the genioglossus and/or tensor veli palatini muscles and based on EEG leads other than C3 and C4.

Supplementary material

Supplementary material is available at *Brain Communications* online.

Acknowledgements

We are particularly grateful to Mrs. Rosie Gilchrist for expert English language editing. Parts of this research were conducted using the supercomputer Mogon and advisory services offered by Johannes Gutenberg University Mainz (hpc.uni-mainz.de), which is a member of the AHRP and the Gauss Alliance e.V. We gratefully acknowledge the computing time granted on Mogon.

Funding

We are gratefully acknowledging the Collaborative Research Center (CRC) 1193, and CRC TR-128 funded by the German research foundation (DFG) and funding by the German Federal Ministry of Economic Affairs and Energy (WIPANO-03THW13K05) and the Boehringer Ingelheim Fonds (BIF-03).

Competing interests

The authors report no competing interests.

References

Amjad AM, Halliday DM, Rosenberg JR, Conway BA. An extended difference of coherence test for comparing and combining several independent coherence estimates: theory and application to the study of motor units and physiological tremor. J Neurosci Methods 1997; 73: 69–79.

Baker SN. Oscillatory interactions between sensorimotor cortex and the periphery. Curr Opin Neurobiol 2007; 17: 649–55.

Berry RB, Budhiraja R, Gottlieb DJ, Gozal D, Iber C, Kapur VK, et al. American Academy of Sleep Medicine. Rules for scoring respiratory events in sleep: update of the 2007 AASM manual for the scoring of sleep and associated events. Deliberations of the sleep apnea

definitions task force of the American Academy of Sleep Medicine. J Clin Sleep Med 2012; 8: 597–619.

Boudewyns AN, Van de Heyning PH, De Backer WA. Site of upper airway obstruction in obstructive apnoea and influence of sleep stage. Eur Respir J 1997; 10: 2566–72.

Carbonnell L, Hasbroucq T, Grapperon J, Vidal F. Response selection and motor areas: a behavioural and electrophysiological study. Clin Neurophysiol 2004; 115: 2164–74.

De Carli F, Proserpio P, Morrone E, Sartori I, Ferrara M, Gibbs SA, et al. Activation of the motor cortex during phasic rapid eye movement sleep. Ann Neurol 2016; 79: 326–30.

Farina D, Merletti R, Enoka RM. The extraction of neural strategies from the surface EMG: an update. J Appl Physiol 2014; 117: 1215–30.

Frauscher B, Gabelia D, Mitterling T, Biermayr M, Bregler D, Ehrmann L, et al. Motor events during healthy sleep: a quantitative polysomnographic study. Sleep 2014; 37: 763–73.

Gabryelska A, Białasiewicz P. Association between excessive daytime sleepiness, REM phenotype and severity of obstructive sleep apnea. Sci Rep 2020; 10: 34.

Gouveris H, Eckert DJ. Editorial: obstructive sleep apnea and the brain. Front Surg 2018; 5: 78.

Halliday DM, Rosenberg JR, Amjad AM, Breeze P, Conway BA, Farmer SF. A framework for the analysis of mixed time series/point process data–theory and application to the study of physiological tremor, single motor unit discharges and electromyograms. Prog Biophys Mol Biol 1995; 64: 237–78.

Jung KY, Cho JH, Ko D, Seok HY, Yoon HK, Lee HJ, et al. Increased corticomuscular coherence in idiopathic REM sleep behavior disorder. Front Neurol 2012; 3: 60. doi: 10.3389/fneur.2012.00060.

Lapatki BG, Oostenveld R, Van Dijk JP, Jonas IE, Zwarts MJ, Stegeman DF. Topographical characteristics of motor units of the lower facial musculature revealed by means of high-density surface EMG. J Neurophysiol 2006; 95: 342–54.

Malhotra A, Fogel RB, Edwards JK, Shea SA, White DP. Local mechanisms drive genioglossus activation in obstructive sleep apnea. Am J Respir Crit Care Med 2000; 161: 1746–9.

Massimini M, Ferrarelli F, Esser SK, Riedner BA, Huber R, Murphy M, et al. Triggering sleep slow waves by transcranial magnetic stimulation. Proc Natl Acad Sci USA 2007; 104: 8496–501.

McSharry DG, Saboisky JP, Deyoung P, Matteis P, Jordan AS, Trinder J, et al. A mechanism for upper airway stability during slow wave sleep. Sleep 2013; 36: 555–63.

Melo-Silva CA, Borel JC, Gakwaya S, Sériès F. Acute upper airway muscle and inspiratory flow responses to transcranial magnetic stimulation during sleep in apnoeic patients. Exp Physiol 2013a; 98: 946–56.

Melo-Silva CA, Gakwaya S, Rousseau E, Sériès F. Consecutive transcranial magnetic stimulation twitches reduce flow limitation during sleep in apnoeic patients. Exp Physiol 2013b; 98: 1366–75.

Mima T, Hallett M. Corticomuscular coherence: a review. J Clin Neurophysiol 1999; 16: 501–11.

Mitra PP, Pesaran B. Analysis of dynamic brain imaging data. Biophys J 1999; 76: 691–708.

Muthuraman M, Galka A, Deuschl G, Heute U, Raethjen J. Dynamical correlation of non-stationary signals in time domain–a comparative study. Biomed Signal Process Control 2010; 5: 205–13.

Muthuraman M, Raethjen J, Koirala N, Anwar AR, Mideksa KG, Elble R, et al. Cerebello-cortical network fingerprints differ between essential, Parkinson's and mimicked tremors. Brain 2018; 141: 1770–81.

Oostenveld R, Fries P, Maris E, Schoffelen JM. FieldTrip: open source software for advanced analysis of MEG, EEG, and invasive electrophysiological data. Comput Intell Neurosci 2011; 2011: 1–9.

Rangayyan RM. Biomedical signal analysis: a case-study approach. Piscataway, NJ: IEEE Press—Wiley Interscience; 2001.

Ratnavadivel R, Chau N, Stadler D, Yeo A, McEvoy RD, Catcheside PG. Marked reduction in obstructive sleep apnea severity in slow wave sleep. J Clin Sleep Med 2009; 05: 519–24.

Ratnavadivel R, Stadler D, Windler S, Bradley J, Paul D, McEvoy RD, et al. Upper airway function and arousability to ventilatory challenge in slow wave versus stage 2 sleep in obstructive sleep apnoea. Thorax 2010; 65: 107–12.

Rosenberg JR, Amjad AM, Breeze P, Brillinger DR, Halliday DM. The Fourier approach to the identification of functional coupling between neuronal spike trains. Prog Biophys Mol Biol 1989; 53: 1–31.

Saboisky JP, Stashuk DW, Hamilton-Wright A, Carusona AL, Campana LM, Trinder J, et al. Neurogenic changes in the upper airway of patients with obstructive sleep apnea. Am J Respir Crit Care Med 2012; 185: 322–9.

Somboon T, Grigg-Damberger M, Foldvary-Schaefer N. Epilepsy and sleep-related breathing disturbances. Chest 2019; 156: 172–81.

Yang Q, Fang Y, Sun CK, Siemionow V, Ranganathan VK, Khoshknabi D, et al. Weakening of functional corticomuscular coupling during muscle fatigue. Brain Res 2009; 1250: 101–12.

Welch PD. The use of fast Fourier transform for the estimation of power spectra: a method based on time averaging over short, modified periodograms. IEEE Trans Audio Electroacoust 1967; 15: 70–3.